

Spin-boson coupling in continuous-time quantum Monte Carlo

Junya Otsuki^{1,2}

¹*Theoretical Physics III, Center for Electronic Correlations and Magnetism,
Institute of Physics, University of Augsburg, D-86135 Augsburg, Germany*

²*Department of Physics, Tohoku University, Sendai 980-8578, Japan*

(Dated: May 16, 2019)

A vector bosonic field coupled to the electronic spin is treated by means of the continuous-time quantum Monte Carlo method. In the Bose Kondo model with a sub-Ohmic density of states $\rho_B(\omega) \sim \omega^{-s}$, two contributions to the spin susceptibility, the Curie term T^{-1} and the term T^{-s} due to bosonic fluctuations, are observed separately. By including the fermionic bath, a quantum phase transition is identified between the Kondo screened state and the bosonic fluctuating state, at which the effective moment and the local Fermi-liquid energy scale vanish. It is demonstrated that the energy scale of the bosonic fluctuation is not affected by the existence of the quantum phase transition.

PACS numbers: 75.20.Hr, 71.10.-w

I. INTRODUCTION

The continuous-time quantum Monte Carlo (CT-QMC) method has been developing since 2005, as a numerical tool for correlated fermion systems.[1, 2] Especially, the algorithm based on the expansion around the atomic limit (CT-HYB) is highly effective as the impurity solver for the dynamical mean-field theory (DMFT).[3–5] The method can also be applied to variants of Kondo models, where a localized spin interacts with the fermionic bath via the exchange coupling.[6, 7]

There is another class of impurity models which consist of an additional coupling between a bosonic bath and local degrees of freedom. The simplest one is the coupling between the electronic charge n_f and a boson ϕ of the form $n_f \phi$. In CT-QMC, arbitrary energy dispersion of the bosonic bath is treatable, and a dynamical screening effect has been investigated.[8] This algorithm can also be applied to the coupling $S_f^z \phi$ with S_f^z being z -component of the local spin.[9] We may consider more complicated interaction including a spin flip scattering of the bosonic field, leading to the coupling $\mathbf{S}_f \cdot \boldsymbol{\phi}$, where a vector bosonic field $\boldsymbol{\phi}$ couples to the electronic spin \mathbf{S}_f .

The coupling $\mathbf{S}_f \cdot \boldsymbol{\phi}$ appears when the Heisenberg interaction is treated in a “mean-field” theory. The boson ϕ describes an auxiliary field which mediates the effective local spin-spin interaction resulting from the intersite interaction. A “mean-field” treatment of the quantum spin glass introduces this interaction with a self-consistent equation.[10–13] In the (non-random) Heisenberg model, this impurity model describes spin fluctuations around the molecular field in magnetic ordered states as well as in the paramagnetic state.[14] With a fermionic bath in terms of DMFT,[15] doping of the spin glass[16] as well as the Heisenberg-Hubbard model can be addressed beyond the molecular-field approximation.[17–19] This extended DMFT equation has recently been reformulated in the dual boson approach.[20] A similar model has also been investigated in the context of a non-magnetic impurity embedded in an antiferromagnet.[21]

The impurity Hamiltonian consisting of the fermionic bath $a_{\mathbf{k}\sigma}$ and the vector bosonic bath $b_{\mathbf{q}\xi}$ ($\xi = x, y, z$) reads

$$H = \sum_{\sigma} \epsilon_{f\sigma} n_{f\sigma} + U n_{f\uparrow} n_{f\downarrow} + \sum_{\mathbf{k}\sigma} \epsilon_{\mathbf{k}} a_{\mathbf{k}\sigma}^{\dagger} a_{\mathbf{k}\sigma} + \sum_{\mathbf{q}\xi} \omega_{\mathbf{q}\xi} b_{\mathbf{q}\xi}^{\dagger} b_{\mathbf{q}\xi} + V \sum_{\sigma} (f_{\sigma}^{\dagger} a_{\sigma} + a_{\sigma}^{\dagger} f_{\sigma}) + \sum_{\xi} g_{\xi} S_f^{\xi} \phi^{\xi}, \quad (1)$$

where $a_{\sigma} = N^{-1/2} \sum_{\mathbf{k}} a_{\mathbf{k}\sigma}$, $\phi^{\xi} = b_{\xi} + b_{\xi}^{\dagger}$, and $b_{\xi} = N^{-1/2} \sum_{\mathbf{q}} b_{\mathbf{q}\xi}$ with N being the number of sites. $n_{f\sigma} = f_{\sigma}^{\dagger} f_{\sigma}$, and $S_f^{\xi} = \sum_{\sigma\sigma'} f_{\sigma}^{\dagger} \sigma^{\xi} f_{\sigma'}$ with σ^{ξ} being the Pauli matrix. We introduce the XXZ-type anisotropy for the bosonic bath and the spin-boson coupling, $\omega_{\mathbf{q}x} = \omega_{\mathbf{q}y} \equiv \omega_{\mathbf{q}\perp}$ and $g_x = g_y \equiv g_{\perp}$.

The bosonic part in H is reminiscent of the spin-boson model, which has been investigated in the context of dissipative systems.[22, 23] Its SU(2) symmetric version is referred to as Bose Kondo model.[21] On the other hand, the model including a spin exchange coupling with the fermionic bath is known as Bose-Fermi Kondo model.[17] The Hamiltonian (1) describes charge fluctuations as well, and may be referred to as Bose-Fermi Anderson model.

The essence of this model is that the fermionic bath screens the localized spin, while the bosonic bath stabilizes the local moment to decouple the fermionic bath. This competition, in a certain situation, leads to a quantum phase transition between the Kondo-screened state for small g and a local-moment state with a residual moment for large g . [24] When the SU(2) symmetry for the spin is preserved, the local-moment state is governed by an intermediate-coupling fixed point.[21] A critical nature has been clarified by means of renormalization group theory with inclusion of full anisotropy.[25–28]

In numerical approach, on the other hand, the case of Ising-type coupling has been investigated by numerical renormalization group (NRG).[29] In this case, the local-moment state is governed by a strong-coupling fixed

point. In this paper, we address the isotropic coupling with SU(2) symmetry and explore the physical quantities arising from the intermediate-coupling fixed point as well as the quantum phase transition.

In the next section, we present an algorithm based on CT-QMC to solve the model (1). We restrict ourselves to $U = \infty$ in the simulation, which is related to the t - J model and the Heisenberg model in terms of the extended DMFT. Numerical results are presented first for a pure bosonic system $V = 0$ (Bose Kondo model) in Sec. III. By including the fermionic bath, the quantum phase transition is explored in Sec. IV. A summary is finally given in Sec. V.

II. SPIN-BOSON COUPLING IN CT-QMC

We solve the effective impurity model (1) using the hybridization-expansion solver of the CT-QMC.[2, 3] In this section, we present how to treat the additional bosonic field in CT-QMC.

The bosonic bath coupled to the electronic charge has been formulated by Werner and Millis[8]. In this method, the electron-phonon coupling is eliminated by the so-called Lang-Firsov transformation, and it makes the computation efficient. This manipulation can also be applied to the coupling between S_f^z and bosons.[9] In the presence of the spin-flip term, however, the above treatment cannot be applied, since the spin operators, S_f^x , S_f^y , and S_f^z , do not commute with each other. Only one component can be eliminated among three. We evaluate the other two couplings by a stochastic method. Namely, hybridization as well as the spin-boson coupling are evaluated via a Monte Carlo sampling.

Before going to the formulation, we define the propagators for the fermionic bath (hybridization function) and the bosonic bath (effective interaction) as follows:

$$\Delta(i\omega_n) = V^2 G_0(i\omega_n) = \frac{V^2}{N} \sum_{\mathbf{k}} \frac{1}{i\omega_n - \epsilon_{\mathbf{k}}}, \quad (2)$$

$$\mathcal{J}_\gamma(i\nu_n) = -g_\gamma^2 D_{\gamma 0}(i\nu_n) = \frac{g_\gamma^2}{N} \sum_{\mathbf{q}} \frac{2\omega_{\mathbf{q}\gamma}}{\nu_n^2 + \omega_{\mathbf{q}\gamma}^2}, \quad (3)$$

where $\omega_n = (2n+1)\pi T$ and $\nu_n = 2n\pi T$ are the fermionic and bosonic Matsubara frequencies and $\gamma = z, \perp$. The latter quantity describes the effective interaction $-\mathbf{S}_f(\tau) \cdot \mathcal{J}(\tau - \tau') \mathbf{S}_f(\tau')$ mediated by the bosonic field.

A. Canonical transformation

We first eliminate the coupling between S_f^z and bosons. Following Ref. [8], we perform a canonical transformation $\tilde{H} = e^{\mathcal{S}} H e^{-\mathcal{S}}$ with $\mathcal{S} = N^{-1/2} \sum_{\mathbf{q}} (g_z/\omega_{\mathbf{q}z})(b_{\mathbf{q}z}^\dagger - b_{\mathbf{q}z}) S_f^z$, which shifts the z -coordinate of the oscillation to eliminate the term $g_z S_f^z \phi^z$. The transformed Hamiltonian \tilde{H}

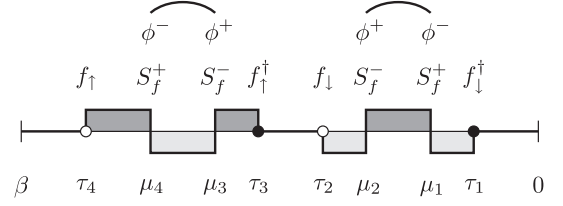


FIG. 1: An example of the Monte Carlo configuration of order $k = 2$ and $l = 2$. The dark and light shaded area indicate the spin-up and -down states, respectively. The curved lines express the bosonic Green function.

is given by

$$\begin{aligned} \tilde{H} = & \sum_{\sigma} \tilde{\epsilon}_{f\sigma} n_{f\sigma} + \tilde{U} n_{f\uparrow} n_{f\downarrow} + \sum_{\mathbf{k}\sigma} \epsilon_{\mathbf{k}} a_{\mathbf{k}\sigma}^\dagger a_{\mathbf{k}\sigma} \\ & + \sum_{\mathbf{q}\xi} \omega_{\mathbf{q}\xi} b_{\mathbf{q}\xi}^\dagger b_{\mathbf{q}\xi} + V \sum_{\sigma} (\tilde{f}_\sigma^\dagger a_\sigma + a_\sigma^\dagger \tilde{f}_\sigma) \\ & + \frac{g_\perp}{\sqrt{2}} (\tilde{S}_f^+ \phi^- + \tilde{S}_f^- \phi^+), \end{aligned} \quad (4)$$

where $\phi^\pm = (\phi^x \pm i\phi^y)/\sqrt{2}$. The local parameters are renormalized to $\tilde{\epsilon}_{f\sigma} = \epsilon_{f\sigma} - N^{-1} \sum_{\mathbf{q}} g_z^2/(4\omega_{\mathbf{q}z})$ and $\tilde{U} = U + N^{-1} \sum_{\mathbf{q}} g_z^2/(2\omega_{\mathbf{q}z})$. The operators for the local electron are transformed to

$$\tilde{f}_\sigma = e^{-\sigma A/2} f_\sigma, \quad \tilde{f}_\sigma^\dagger = e^{\sigma A/2} f_\sigma^\dagger, \quad \tilde{S}_f^\pm = e^{\pm A} S_f^\pm, \quad (5)$$

where $S_f^\pm = S_f^x \pm iS_f^y$ and $A = N^{-1/2} \sum_{\mathbf{q}} (g_z/\omega_{\mathbf{q}z})(b_{\mathbf{q}z}^\dagger - b_{\mathbf{q}z})$. In Eq. (5), the factor $e^{A/2}$ is associated with the change in the quantum number of S_f^z .

B. Partition function

With the transformed Hamiltonian \tilde{H} , we expand the partition function Z with respect to V and g_\perp as follows:

$$\frac{Z}{Z_0} = \sum_{k=0}^{\infty} \sum_{l=0}^{\infty} \int d\boldsymbol{\tau} \int d\boldsymbol{\mu} W(\boldsymbol{\tau}, \boldsymbol{\mu}), \quad (6)$$

where the subscript 0 denotes a quantity for $V = g_\perp = 0$. The integrand $W(\boldsymbol{\tau}, \boldsymbol{\mu})$ describes the contribution of order $V^{2k} g_\perp^{2l}$. $\boldsymbol{\tau} = (\tau_1, \dots, \tau_{2k})$ denotes a set of imaginary times at which the hybridization events occur. The integral over $\boldsymbol{\tau}$ is taken for the range $\beta > \tau_{2k} > \dots > \tau_1 \geq 0$. $\boldsymbol{\mu} = (\mu_1, \dots, \mu_{2l})$ denotes a set of imaginary times at which a spin exchange takes place. The integral over $\boldsymbol{\mu}$ is taken in the same manner as $\boldsymbol{\tau}$. Figure 1 shows an example of the configuration. The doubly occupied state is excluded in this figure, since we consider the limit $U = \infty$ in the next subsection. We note that the formulae in this subsection are valid also for $U < \infty$. In the simulation, the summations over k and l as well as the integrals over $\boldsymbol{\tau}$ and $\boldsymbol{\mu}$ are to be evaluated via the importance sampling.

The weight $W(\boldsymbol{\tau}, \boldsymbol{\mu})$ is decoupled into four contributions:

$$W(\boldsymbol{\tau}, \boldsymbol{\mu}) = \tilde{W}_{\text{loc}}(\boldsymbol{\tau}, \boldsymbol{\mu}) W_{\text{hyb}}(\boldsymbol{\tau}) W_{\perp}(\boldsymbol{\mu}) W_z(\boldsymbol{\tau}, \boldsymbol{\mu}). \quad (7)$$

They denote, from left to right, thermal averages over the f -state, the fermionic bath, the xy -component of the bosonic bath, and the z -component. The first two are the contributions from the Anderson model:[3] \tilde{W}_{loc} is the trace over the f -states with the renormalized parameters, $\tilde{\epsilon}_{f\sigma}$ and \tilde{U} , and W_{hyb} is the trace over the fermionic bath, which is expressed by the determinant of $k \times k$ matrix consisting of $\Delta(\tau)$ in Eq. (2).

$W_{\perp}(\boldsymbol{\mu})$ describes the contribution from the g_{\perp} -terms and is given by

$$W_{\perp}(\boldsymbol{\mu}) = \frac{g_{\perp}^{2l}}{2^l} \langle \phi^{\eta_{2l}}(\mu_{2l}) \cdots \phi^{\eta_1}(\mu_1) \rangle_0, \quad (8)$$

where ϕ^{η} denotes either ϕ^+ or ϕ^- . The numbers of ϕ^+ and ϕ^- must be the same since we have the relation $\langle \phi^{\pm}(\mu_i) \phi^{\pm}(\mu_j) \rangle_0 = 0$. The thermal average in W_{\perp} is decomposed by Wick's theorem, which is represented by the permanent of $l \times l$ matrix consisting of $D_{\perp 0}(\mu_i - \mu_j) = -\langle T_{\tau} \phi^+(\mu_i) \phi^-(\mu_j) \rangle_0$. [30] However, since there is no efficient algorithm to compute the permanent, we evaluate it by stochastic sampling.[31] Namely, we express W_{\perp} as

$$W_{\perp}(\boldsymbol{\mu}) = \sum_{\alpha} W_{\perp}(\boldsymbol{\mu}; \alpha), \quad (9)$$

with α denoting one of terms in the permanent, and the summation is to be evaluated stochastically. In Fig. 1, the configuration α is represented by curved lines.

$W_z(\boldsymbol{\tau}, \boldsymbol{\mu})$ consists of the phase factors in Eq. (5) and is represented as

$$W_z(\boldsymbol{\tau}, \boldsymbol{\mu}) = \langle e^{s_{2m} A(t_{2m})} \cdots e^{s_1 A(t_1)} \rangle_0, \quad (10)$$

where $\{t_i\}$ is composed of $\boldsymbol{\tau}$ and $\boldsymbol{\mu}$ in ascending order and $m = k + l$. $A(t) = N^{-1/2} \sum_{\mathbf{q}} (g_z / \omega_{\mathbf{q}z}) (e^{\omega_{\mathbf{q}z} t} b_{\mathbf{q}z}^{\dagger} - e^{-\omega_{\mathbf{q}z} t} b_{\mathbf{q}z})$. The factor s_i takes $\sigma/2$ for f_{σ}^{\dagger} , $-\sigma/2$ for f_{σ} , and ± 1 for S_f^{\pm} . Using the condition $\sum_i s_i = 0$, the thermal average can be evaluated analytically to give[8]

$$W_z(\boldsymbol{\tau}, \boldsymbol{\mu}) = \exp \left[\sum_{2m \geq j > i \geq 1} s_i s_j K(t_j - t_i) \right], \quad (11)$$

$$K(\tau) = -\frac{1}{N} \sum_{\mathbf{q}} \frac{g_z^2}{\omega_{\mathbf{q}z}^2} [B(\omega_{\mathbf{q}z}, \tau) - B(\omega_{\mathbf{q}z}, 0)], \quad (12)$$

where $B(\omega, \tau) = \cosh[(\beta/2 - \tau)\omega] / \sinh(\beta\omega/2)$.

The dynamics of the bosonic bath is described by the function $\mathcal{J}_{\gamma}(i\nu_n)$ defined in Eq. (3). It is therefore convenient to express the summations over \mathbf{q} in the above formulae in terms of $\mathcal{J}_{\gamma}(i\nu_n)$. The renormalized parameters are rewritten as $\tilde{\epsilon}_{f\sigma} = \epsilon_{f\sigma} - \mathcal{J}_z(0)/8$ and

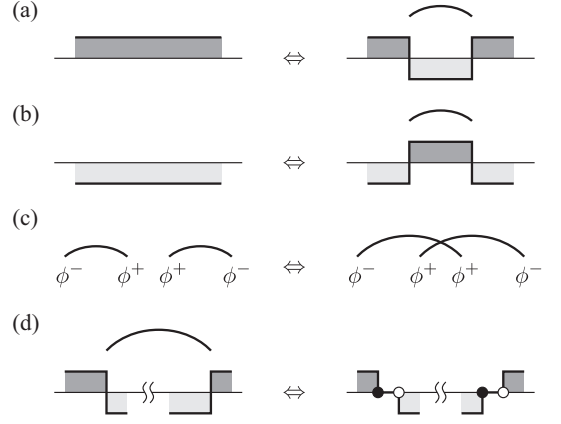


FIG. 2: Update processes necessary to evaluate the spin-boson coupling.

$\tilde{U} = U + \mathcal{J}_z(0)/4$. On the other hand, $K(\tau)$ in Eq. (12) is expressed as

$$K(\tau) = \mathcal{J}_z(0) \frac{\tau(\beta - \tau)}{2\beta} - \sum_{n \neq 0} \mathcal{J}_z(i\nu_n) \frac{1 - \cos \tau \nu_n}{\beta \nu_n^2}. \quad (13)$$

C. Monte Carlo procedure

We perform stochastic samplings of $\boldsymbol{\tau}$ and $\boldsymbol{\mu}$ in Eq. (6) and α in Eq. (9). They respectively correspond to the V -expansion, g_{\perp} -expansion and the Wick's theorem for the bosonic field. Since the Hamiltonian with $V = g_{\perp} = 0$ conserves the quantum number of S_f^z , we can treat \tilde{W}_{loc} by the “segment picture” of CT-HYB.[2, 3] Hence for the V -expansion, the update procedure in the Anderson model can be used.[8] Hereafter, we consider the limit $U = \infty$, which can be implemented by excluding the doubly occupied state in the configuration.

In addition to the updates in CT-HYB, we perform the following updates:

- (a) Insertion/Removal of $S_f^+(\mu + \ell) S_f^-(\mu)$ on \uparrow -state.
- (b) Insertion/Removal of $S_f^-(\mu + \ell) S_f^+(\mu)$ on \downarrow -state.
- (c) Change of the configuration α .
- (d) Replacing $S_f^+(\mu'_i)$ and $S_f^-(\mu_i)$ with $f_{\uparrow}^{\dagger}(\mu'_i + \ell') f_{\downarrow}(\mu'_i)$ and $f_{\downarrow}^{\dagger}(\mu_i + \ell) f_{\uparrow}(\mu_i)$, and vice versa.

These updates are expressed diagrammatically in Fig. 2. The updates (a) and (b) change the expansion order of g_{\perp} by 2. In (c), we exchange two links of the bosonic Green functions. The ergodicity is in principle satisfied only by (a)–(c). However, a part of the configuration may freeze in practice, when the expansion orders for g_{\perp} and V are considerably different from each other, say, when g_{\perp} is much smaller than V . The freezing happens

because the spin operators are separated with each other by hybridization operators being located in between. In such a situation, the spin operators cannot be removed by the updates (a) and (b). This problem can be resolved by introducing the update (d), which replaces two spin operators separated in the time ordering by single-particle operators. [For example, this update is important in the parameter range $0 < g \lesssim 0.12$ in Fig. 6.]

We first consider the update (a). In the insertion process, we choose two imaginary times randomly in the same way as the “segment algorithm”[2, 3]: μ is first chosen from the range $[0 : \beta)$ and then the length ℓ is chosen in the range $(0 : \ell_{\max})$ so that the operator S_f^+ does not pass the next operators. In the removal process, we choose one pair from $(l + 1)$ pairs of the spin operators which are connected by the bosonic line, and try the update if it is allowed, i.e., if no operator exists between them. From the detailed balance condition, the update probability R is given by

$$R(\boldsymbol{\mu} \rightarrow \boldsymbol{\mu}^+) = \frac{\beta \ell_{\max}}{l + 1} \frac{\mathcal{J}_{\perp}(-\ell)}{2} \frac{\tilde{W}_{\text{loc}}(\boldsymbol{\tau}, \boldsymbol{\mu}^+)}{\tilde{W}_{\text{loc}}(\boldsymbol{\tau}, \boldsymbol{\mu})} \frac{W_z(\boldsymbol{\tau}, \boldsymbol{\mu}^+)}{W_z(\boldsymbol{\tau}, \boldsymbol{\mu})}, \quad (14)$$

where $\boldsymbol{\mu}$ and $\boldsymbol{\mu}^+$ denote the configurations of order g_{\perp}^{2l} and $g_{\perp}^{2(l+1)}$, respectively. The expression for the update (b) is given in a similar manner.

The update probability for (c) comes only from W_{\perp} . Suppose that (μ_i, μ'_i) and (μ_j, μ'_j) denote the pairs of imaginary times connected by the bosonic Green function in the original configuration α , the update probability R of exchanging the links is given by

$$R(\alpha \rightarrow \alpha') = \frac{\mathcal{J}_{\perp}(\mu_i - \mu'_j) \mathcal{J}_{\perp}(\mu_j - \mu'_i)}{\mathcal{J}_{\perp}(\mu_i - \mu'_i) \mathcal{J}_{\perp}(\mu_j - \mu'_j)}. \quad (15)$$

Finally, we consider the update (d). We first choose a pair of spin operators connected by the bosonic line, as in the removal process in the update (a). They are to be replaced by f_{\downarrow} and f_{\uparrow} , respectively. Simultaneously, the operator f_{\uparrow}^{\dagger} (f_{\downarrow}^{\dagger}) is placed next to f_{\downarrow} (f_{\uparrow}). Here, the length of the empty state ℓ (ℓ') is chosen from the range up to ℓ_{\max} (ℓ'_{\max}) so that the resultant configuration is allowed. In the opposite process, we choose the operators f_{\downarrow} and f_{\uparrow} from $(k_{\downarrow} + 1)$ and $(k_{\uparrow} + 1)$ randomly, where k_{σ} denotes the hybridization-expansion order for spin σ . The update probability R is given by

$$R(\boldsymbol{\tau}, \boldsymbol{\mu} \rightarrow \boldsymbol{\tau}^{++}, \boldsymbol{\mu}^-) = \frac{\ell \ell'_{\max}}{(k_{\uparrow} + 1)(k_{\downarrow} + 1)} \frac{2}{\mathcal{J}_{\perp}(\mu_i - \mu'_i)} \times \frac{W_{\text{hyb}}(\boldsymbol{\tau}^{++})}{W_{\text{hyb}}(\boldsymbol{\tau})} \frac{\tilde{W}_{\text{loc}}(\boldsymbol{\tau}^{++}, \boldsymbol{\mu}^-)}{\tilde{W}_{\text{loc}}(\boldsymbol{\tau}, \boldsymbol{\mu})} \frac{W_z(\boldsymbol{\tau}^{++}, \boldsymbol{\mu}^-)}{W_z(\boldsymbol{\tau}, \boldsymbol{\mu})}, \quad (16)$$

where $\boldsymbol{\tau}^{++}$ and $\boldsymbol{\mu}^-$ denote the new configuration of order $V^{2(k+2)} g_{\perp}^{2(l-1)}$.

We have confirmed, in the simulation, that all the update probabilities presented above are always positive and therefore, the simulation does not suffer from the sign problem.

D. Spin susceptibility

We define the spin susceptibilities by $\chi_{zz}(\tau) = \langle S_f^z(\tau) S_f^z \rangle$ and $\chi_{+-}(\tau) = \langle S_f^+(\tau) S_f^- \rangle / 2$. In the isotropic system, we have $\chi_{zz}(\tau) = \chi_{+-}(\tau)$. We can evaluate $\chi_{zz}(\tau)$ from the configuration of the f -operators as in the “segment algorithm”[2, 3]. On the other hand, $\chi_{+-}(\tau)$ can be evaluated by

$$\chi_{+-}(\tau) = T \left\langle \sum_{i=1}^l \frac{\delta(\tau, \mu'_i - \mu_i)}{\mathcal{J}_{\perp}(\mu_i - \mu'_i)} \right\rangle_{\text{MC}}, \quad (17)$$

where μ_i and μ'_i denote the imaginary times for S_f^- and S_f^+ which are connected by the bosonic Green function, and MC means average over Monte Carlo configuration. The function $\delta(\tau, \mu)$ is defined by

$$\delta(\tau, \mu) = \begin{cases} \delta(\tau - \mu) & (\mu > 0) \\ \delta(\tau - \mu - \beta) & (\mu < 0) \end{cases}, \quad (18)$$

and $\chi_{+-}(\tau)$ is sampled in the range $0 < \tau < \beta$. The end points are evaluated accurately from the occupation number using the relations $\chi_{+-}(+0) = \langle n_{f\uparrow} \rangle / 2$ and $\chi_{+-}(\beta - 0) = \langle n_{f\downarrow} \rangle / 2$. Eq. (17) follows from the fact that \mathcal{J}_{\perp} describes the retarded interaction between the local spin so that it may be regarded as the source field for the susceptibility.

The susceptibilities $\chi_{zz}(\tau)$ and $\chi_{+-}(\tau)$ can also be computed using the matrix M_{σ} which is kept in the simulation to evaluate the determinant in W_{hyb} . [1–3] Although this way is not efficient compared to the method presented above, we can use it for a check of the algorithm and a code. Another consistency check is $\chi_{zz}(\tau) = \chi_{+-}(\tau)$ in isotropic parameters, since this condition is not trivial in the present algorithm, which treats g_z and g_{\perp} in different ways. We have confirmed that our results satisfy this condition.

III. PURE BOSONIC SYSTEM

In this section, we present numerical results for the pure bosonic system, $V = 0$. In our simulation, the charge fluctuation is absent because of $U = \infty$ so that the local electron is reduced to a localized spin \mathbf{S} . Hence, the corresponding Hamiltonian is written as

$$H_{\text{BK}} = \sum_{\mathbf{q}} \omega_{\mathbf{q}} \mathbf{b}_{\mathbf{q}}^{\dagger} \cdot \mathbf{b}_{\mathbf{q}} + g \mathbf{S} \cdot \boldsymbol{\phi}. \quad (19)$$

This model is referred to as Bose Kondo model, which has been investigated in the context of an impurity embedded in an antiferromagnet.[21, 25] We restrict ourselves to the isotropic system, $\omega_{\mathbf{q}z} = \omega_{\mathbf{q}\perp} \equiv \omega_{\mathbf{q}}$ and $g_z = g_{\perp} \equiv g$.

The bosonic bath is characterized by the density of states $\rho_{\text{B}}(\omega) = N^{-1} \sum_{\mathbf{q}} \delta(\omega - \omega_{\mathbf{q}})$. We use a function $\rho_{\text{B}}(\omega) \propto \omega^s$ with a cut-off energy ω_c . The sum-rule of

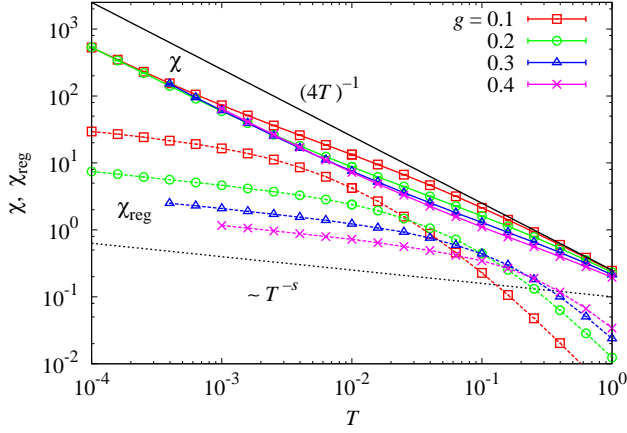


FIG. 3: (Color online) Temperature dependences of the static susceptibility $\chi(0)$ in the pure bosonic system with $s = 0.2$ (solid lines). The regular part $\chi_{\text{reg}}(0)$ defined in Eq. (21) is also plotted (dashed lines).

the density of states, $\int_0^\infty d\omega \rho_B(\omega) = 1$, determines the factor to yield the explicit form

$$\rho_B(\omega) = (s+1)\omega^s \omega_c^{-s-1} \theta(\omega_c - \omega). \quad (20)$$

We take $\omega_c = 1$ as the unit of energy.

According to the renormalization group analysis,[21, 25, 27, 28] this model has an intermediate fixed point $g = g^*$ for $0 < s < 1$. At this fixed point, the susceptibility shows the long-time behavior $\chi(\tau) \sim \tau^{1-s}$, which indicates the static susceptibility of the form $\chi \sim T^{-s}$. For $s \geq 1$, on the other hand, the bosonic coupling is irrelevant. We investigate properties due to the intermediate fixed point restricting ourselves to $s = 0.2$.

Fig. 3 shows temperature dependences of the static spin susceptibility for $s = 0.2$. We see the Curie behavior $\chi \propto T^{-1}$ at low temperature indicating existence of a residual moment. To see the singularity T^{-s} originating from the intermediate fixed point, we define a regular part of the susceptibility, $\chi_{\text{reg}}(z)$, by an analytical continuation of $\chi(z = i\nu_n)$ with $\nu_n > 0$. Using $\chi_{\text{reg}}(z)$, the susceptibility is written as

$$\chi(i\nu_n) = \delta_{n0}M/4T + \chi_{\text{reg}}(i\nu_n). \quad (21)$$

We note that the effective moment M may depend on temperature. The full-moment corresponds to $M = 1$. We evaluate $\chi_{\text{reg}}(0)$ by an extrapolation from $\chi(i\nu_1)$, $\chi(i\nu_2)$ and $\chi(i\nu_3)$ with a quadratic function. We have confirmed that the choice of the functional form in the extrapolation does not affect the low-temperature behavior.[32] The result is shown in Fig. 3. We clearly see the power-law behavior $\chi_{\text{reg}}(0) \propto T^{-s}$ at low temperatures. Consequently, the low-temperature static susceptibility can be expressed in terms of two diverging terms

$$\chi(0) \simeq M_0/4T + 1/[4T^s(T_B)^{1-s}], \quad (22)$$

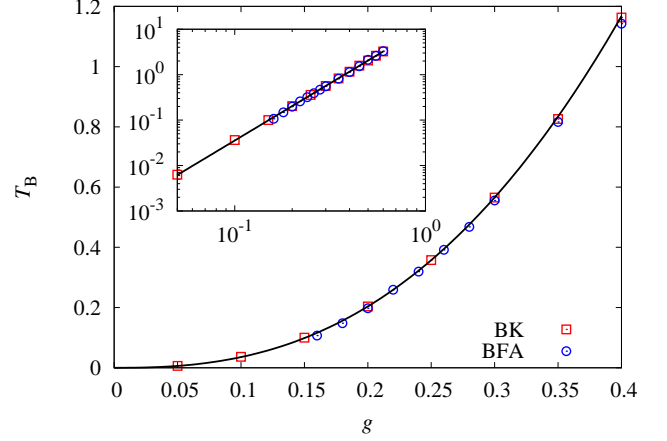


FIG. 4: (Color online) The energy scale T_B of the bosonic fluctuation in the pure bosonic system with $s = 0.2$ (denoted by BK). The result for the Bose-Fermi Anderson model is also plotted (denoted by BFA, see Fig. 5 for parameters). The solid line is the function $T_B \propto g^\alpha$ fitted to the BK data.

where $M_0 = \lim_{T \rightarrow 0} M$ is the residual moment and we have introduced a characteristic energy scale T_B of the bosonic fluctuation. It turns out that T_B exhibits a power-law behavior as shown in Fig. 4. The exponent α defined by $T_B \propto g^\alpha$ is obtained as $\alpha \simeq 2.52$ with the error 0.01. The residual moment M_0 weakly depends on g . [The figure is presented in the next section (Fig. 6) together with results for the Bose-Fermi Anderson model.]

IV. FERMIONIC AND BOSONIC BATHS

We proceed to system with the bosonic and fermionic baths. For the bosonic bath, we fix $s = 0.2$ as in the previous section. For the fermionic density of states, $\rho_F(\omega) = N^{-1} \sum_{\mathbf{k}} \delta(\omega - \epsilon_{\mathbf{k}})$, on the other hand, we use a rectangular model with a cut-off energy D

$$\rho_F(\omega) = (1/2D)\theta(D - |\omega|). \quad (23)$$

We vary $g_z = g_\perp \equiv g$ fixing $V^2 = 0.1$, $\epsilon_{f\sigma} = -0.2$, $U = \infty$ and $\omega_c = D = 1$. The Kondo temperature T_K is estimated to be $T_K \sim 0.1$ for $g = 0$.

According to the renormalization group analysis for the Bose-Fermi Kondo model,[25, 27, 28] there are two fixed points which are stable within $SU(2)$ symmetry in (J, g) plane, where $J \equiv V^2/|\epsilon_{f\sigma}|$ in the present model. One is the fermionic fixed point with $(J, g) = (\infty, 0)$, at which the bosonic bath is decoupled to form the Kondo state. The other is bosonic fluctuating fixed point with $(J, g) = (0, g^*)$, which has been examined in the previous section. A quantum phase transition takes place between these two states. At the critical point, the susceptibility shows the power-law behavior $\chi \sim T^s$.

We show temperature dependence of the spin susceptibility in Fig. 5. Difference with the pure bosonic sys-

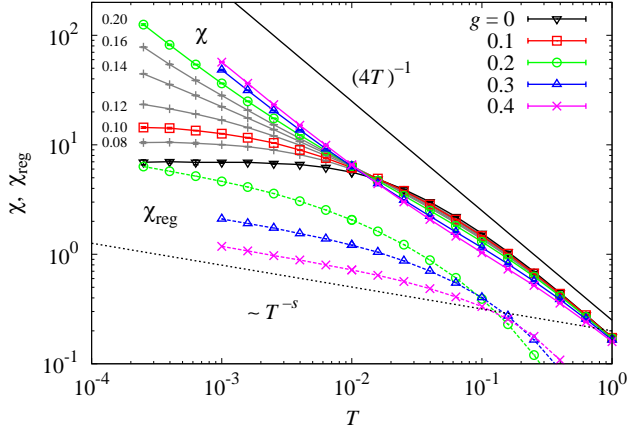


FIG. 5: (Color online) Temperature dependences of the static susceptibility $\chi(0)$ in the Bose-Fermi Anderson model with $V^2 = 0.1$, $\epsilon_{f\sigma} = -0.2$, $U = \infty$ and $s = 0.2$ (solid lines). The dashed lines show the regular part $\chi_{\text{reg}}(0)$ defined in Eq. (21).

tem is the paramagnetic behavior in the small- g region, $g \lesssim 0.10$. This indicates the spin fluctuation in the Kondo singlet state given by[33]

$$\chi(0) = 1/4T_F, \quad (24)$$

with T_F being the energy scale of low-energy excitations. The susceptibility increases against g indicating a reduction of T_F . To quantify the local Fermi-liquid state, we evaluate the renormalization factor z defined by $z = [1 - \text{Im}\Sigma_f(i\omega_0)/\omega_0]^{-1}$. The result is plotted in Fig. 6 for several values of T . A reduction of z with increasing g is demonstrated and at $g = 0.12$ (0.14), it is estimated as $z \leq 0.023$ (0.008). However, since z is not converged around $g = 0.12$ in this temperature range, we cannot identify the quantum critical point from this data.

In the large- g region, $g \gtrsim 0.14$, on the other hand, χ shows the Curie behavior $\chi \propto T^{-1}$. As in the pure bosonic system, we evaluate the regular part $\chi_{\text{reg}}(0)$ defined in Eq. (21), which expresses the contribution excepting the Curie term. It turns out from Fig. 5 that $\chi_{\text{reg}}(0)$ shows the power-law behavior T^{-s} as in Fig. 3. A remarkable point is that the energy scale T_B of the bosonic fluctuation is not affected by the fermionic bath as shown in Fig. 4. Hence, the difference to the pure bosonic system in the local-moment regime comes from the Curie term. To see this, we evaluate the effective moment M by subtracting χ_{reg} from χ in Eq. (21), and plot it as a function of g in Fig. 6. It turns out that M is strongly suppressed compared to that in the pure bosonic system below $g \simeq 0.20$.

Finally, in order to identify the quantum critical point g_c , we plot $T^s\chi$ as a function of g for different temperatures in Fig. 7. The low-temperature expression of χ in Eqs. (22) and (24) indicates that $T^s\chi$ is independent of

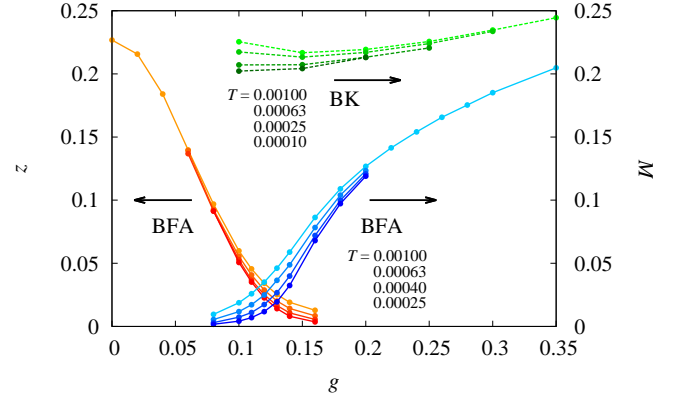


FIG. 6: (Color online) The renormalization factor z and the effective moment M for the parameters same as in Fig. 5. Results at four different temperatures are plotted. The dashed line (denoted by BK) is the result for the pure bosonic system.

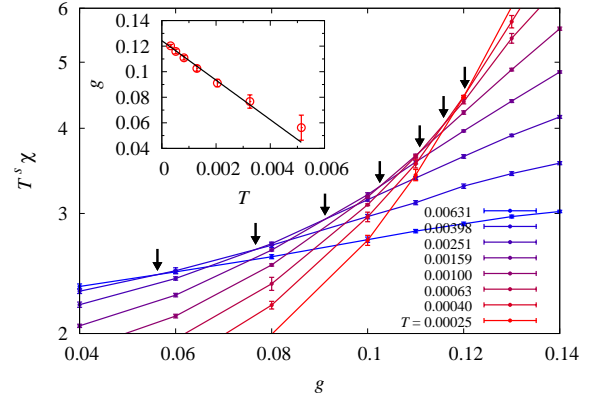


FIG. 7: (Color online) $T^s\chi$ as a function of g for different values of T . From the intersection points, which are indicated by arrows, the critical point is determined. The inset shows extrapolation of the intersection point to $T = 0$.

temperature at $g = g_c$, while $T^s\chi = 0$ for $g < g_c$ and $T^s\chi = \infty$ for $g > g_c$ at $T = 0$. Hence, the intersection of lines for different temperatures gives an estimation of g_c . By extrapolating the crossing point to $T = 0$, we obtain $g_c \simeq 0.124$ with the error 0.001.

V. SUMMARY

We have developed an algorithm of CT-QMC for models including the spin-boson coupling, i.e., the Bose Kondo model and the Bose-Fermi Anderson model. In the Bose Kondo model, we have observed the low-temperature static susceptibility consisting of the Curie term T^{-1} and the bosonic fluctuating term T^{-s} . By including the fermionic bath, i.e., in the Bose-Fermi Anderson model, we have identified the quantum phase transi-

tion between the bosonic fluctuating state and the Kondo singlet state. At the critical point, the quasiparticle energy scale and the effective moment vanish from each side of g . On the other hand, the energy scale of the bosonic fluctuation is not affected by the fermionic bath. As a result, the static susceptibility exhibits the power-law singularity $\chi \propto T^{-s}$ as the leading term at the critical point.

In this paper, we have restricted ourselves to $U = \infty$ in the simulation. However, the formalism for the partition function, or the weight $W(\tau, \mu)$, holds also for $U < \infty$, so that only the update procedure should be modified

to take account of the doubly occupied state. One can also apply the present framework to the Kondo limit, i.e., Bose-Fermi Kondo model. In this case, the algorithm for the Kondo model (CT-J) is available.[2, 6]

The present method can apply to lattice models such as the Heisenberg model and the t - J model in terms of the extended DMFT equation. An application to lattice models as well as a detailed investigation of the impurity models are left for future issues.

The author is supported by JSPS Postdoctoral Fellowships for Research Abroad.

-
- [1] A.N. Rubtsov, V.V. Savkin and A.I. Lichtenstein, Phys. Rev. B **72**, 035122 (2005).
 - [2] For a review, see E. Gull, A. J. Millis, A. I. Lichtenstein, A. N. Rubtsov, M. Troyer, and P. Werner, Rev. Mod. Phys. **83**, 349 (2011).
 - [3] P. Werner, A. Comanac, L. de' Medici, M. Troyer, and A. J. Millis, Phys. Rev. Lett. **97**, 076405, (2006); P. Werner and A. J. Millis, Phys. Rev. B **74**, 155107 (2006).
 - [4] K. Haule, Phys. Rev. B **75**, 155113 (2007).
 - [5] A. M. Läuchli and P. Werner, Phys. Rev. B **80**, 235117 (2009).
 - [6] J. Otsuki, H. Kusunose, P. Werner and Y. Kuramoto, J. Phys. Soc. Jpn. **76**, 114707 (2007).
 - [7] S. Hoshino, J. Otsuki, and Y. Kuramoto, J. Phys. Soc. Jpn. **78**, 074719 (2009).
 - [8] P. Werner and A. J. Millis, Phys. Rev. Lett. **99**, 146404 (2007); P. Werner and A. J. Millis, Phys. Rev. Lett. **104**, 146401 (2010).
 - [9] J. H. Pixley, S. Kirchner, M.T. Glossop, Q. Si, J. Phys.: Conf. Series **273**, 012050 (2011).
 - [10] A. J. Bray and M. A. Moore, J. Phys. C: Solid State Phys. **13**, L655 (1980).
 - [11] D. R. Grempel and M. J. Rozenberg, Phys. Rev. Lett. **80**, 389 (1998).
 - [12] A. Georges, O. Parcollet, and S. Sachdev, Phys. Rev. Lett. **85**, 840 (2000); Phys. Rev. B **63**, 134406 (2001).
 - [13] S. Sachdev and J. Ye, Phys. Rev. Lett. **70**, 3339 (1993).
 - [14] Y. Kuramoto and N. Fukushima, J. Phys. Soc. Jpn. **67**, 583 (1998); N. Fukushima and Y. Kuramoto, J. Phys. Soc. Jpn. **67**, 2460 (1998).
 - [15] A. Georges, G. Kotliar, W. Krauth and M. J. Rozenberg, Rev. Mod. Phys. **68**, 13 (1996).
 - [16] O. Parcollet and A. Georges, Phys. Rev. B **59**, 5341 (1999).
 - [17] J. L. Smith and Q. Si, Phys. Rev. B **61**, 5184 (2000).
 - [18] K. Haule, A. Rosch, J. Kroha, and P. Wölfle, Phys. Rev. Lett. **89**, 236402 (2002); Phys. Rev. B **68**, 155119 (2003).
 - [19] P. Sun and G. Kotliar, Phys. Rev. B **66**, 085120 (2002).
 - [20] A. N. Rubtsov, M. I. Katsnelson, and A. I. Lichtenstein, Ann. Phys. **327**, 1320 (2012).
 - [21] M. Vojta, C. Buragohain, and S. Sachdev, Phys. Rev. B **61**, 15152 (2000).
 - [22] A. J. Leggett, S. Chakravarty, A. T. Dorsey, A. Garg, and W. Zwerger, Rev. Mod. Phys. **59**, 1 (1987).
 - [23] R. Bulla, H.-J. Lee, N.-H. Tong, and M. Vojta, Phys. Rev. B **71**, 045122 (2005).
 - [24] Q. Si, S. Rabello, K. Ingersent, and J. L. Smith, Nature (London) **413**, 804 (2001).
 - [25] For a review, see M. Vojta, Philos. Mag. **86**, 1807 (2006).
 - [26] A. M. Sengupta, Phys. Rev. B **61**, 4041 (2000).
 - [27] L. Zhu and Q. Si, Phys. Rev. B **66**, 024426 (2002).
 - [28] G. Zaránd and E. Demler, Phys. Rev. B **66**, 024427 (2002).
 - [29] M. T. Glossop and K. Ingersent, Phys. Rev. Lett. **95**, 067202 (2005); Phys. Rev. B **75**, 104410 (2007).
 - [30] Although the Hamiltonian (1) leads to the symmetry $\langle T_\tau \phi^+(\tau) \phi^-(\tau) \rangle_0 = \langle T_\tau \phi^-(\tau) \phi^+(\tau) \rangle_0$, we do not use it in the formulation. Hence, all the expressions below are valid also for the case $\langle T_\tau \phi^+(\tau) \phi^-(\tau) \rangle_0 \neq \langle T_\tau \phi^-(\tau) \phi^+(\tau) \rangle_0$.
 - [31] P. Anders, E. Gull, L. Pollet, M. Troyer, and P. Werner, New J. Phys. **13**, 075013 (2011).
 - [32] If we use the inverse of a quadratic function for the extrapolation, the convergence to a low-temperature value is faster, but the result is more sensitive to statistical errors except for low temperatures. The same is true of the Pade approximation.
 - [33] See for example, A. C. Hewson, *The Kondo problem to heavy fermions* (Cambridge University Press, Cambridge, 1993).